ISSN 1 746-7233, England, UK
World Journal of Modelling and Simulation
Vol. 9 (2013) No. 3, pp. 181-191

Transient scattering by conductor bodies: A comparison of Time-Domain computational methods

Ravi Srinivasa Rao[1*], Potluri Venkata Subbaiah[2], Bhima Prabhakara Rao[3]

[1] Department of Electrical and Computer Engineering, Sree Vidyaniketan Engineering College (SVEC), J.N.T.University Ananthapur, Tirupathi 517102, Andhra Pradesh, India
[2] Amrita Sai Institute Science and Technology, J.N.T.University Kakinada, Paritala, Krishna Dist 521180, Andhra Pradesh, India
[3] Department of Electrical and Computer Engineering, University College of Engineering, J.N.T.University Kakinada, Kakinada, East Godavari Dist 533003, Andhra Pradesh, India

(*Received July 24 2012, Revised December 10 2012, Accepted July 05 2013*)

Abstract. Presented in this paper is a comparison of the three popular time domain numerical techniques, viz., the Time-Domain Integral Equation (TDIE) method, the Finite Difference Time Domain method (FDTD) and the Transmission Line Modeling (TLM) method when applied for transient electromagnetic scattering problems. These three popular techniques are useful for signature analysis of direct scattering problem in time domain i.e., finding the scattered field when the incident waveform and the target geometry are given. Even though all of them are time domain techniques, their modeling philosophy is quite different. The TDIE method is based on well known method of moments and in FDTD Maxwell's equations are solved using a differencing scheme. The TLM uses a scattering approach akin to Huygens principle, implemented by replacing the space medium with a system of interconnected transmission-lines. The comparison is made via conductor bodies of standard canonical shapes like a square plate, a pie-plate, a cube, and a sphere, to address the factors affecting accuracy, efficiency, and the required computer resources.

Keywords: Time-Domain Integral Equation method, Moment method, Finite Difference Time Domain method, Transmission Line Modeling method, Symmetrical Condensed Node

1 Introduction

With the advent of sub-nanosecond technology, it became clear that the electromagnetic signature computations, by virtue of digital computer advances, were possible directly in the time domain. The calculations are carried out by illuminating the target with a smoothed-impulse waveform. The resulting smoothed-impulse response contains all the information about the electromagnetic scattering properties of the target over the frequency band that is defined by the spectrum of the incident smoothed impulse.

Several numerical modeling methods for solving electromagnetic problems have been developed. Methods can be classified into generic groups based on the domain of the variable (time or frequency) and the domain of the operator (differential or integral). In dealing with the most general material and conductor configurations at a wide band of high frequencies, integral and differential time-domain techniques[3, 4] offer the most versatile simulation tools.

The foremost methods in this area are the Time-Domain Integral Equation (TDIE)[11] method, Finite-Difference Time-Domain (FDTD)[1] method and Transmission Line Modeling (TLM)[6] method. One of the principal advantages of any time domain technique when compared to frequency domain analysis is their ability to model the electromagnetic fields in an arbitrary geometry over a broad frequency range. While the

* Corresponding author. *E-mail address*: rsrao55@hotmail.com.

TDIE is based on well known Moment method, the FDTD method is Maxwell's equations based approximate mathematical model and TLM method is a physical model based on Huygens' Principle, being implemented with a system of interconnected lines. The use of Symmetrical Condensed Node (SCN) is well established for the solution of complex electromagnetic field problems with TLM method.

These techniques have been used widely to solve the open region problems in the analysis of electromagnetic scattering apart from other types of problems. When applied to open region problems, FDTD as well TLM as techniques require a suitable Absorbing Boundary Condition (ABC). Frequently used ABC is Perfectly Matched Layer (PML) in FDTD method and one-way equation based boundary conditions in TLM method. TDIE is an integral equation based technique which incorporates radiation condition in the formulation itself and hence doesn't require any ABC explicitly implemented.

In all the three methods, the far fields are obtained from the near fields via currents thus obtained. The FDTD and TLM methods use equivalence principle to obtain currents over a rectangular imaginary surface enclosing the scattering object.

A brief comparison is made by Sachdev and Rao[8] between TDIE and FDTD. However, to the best of our knowledge, a thorough comparison of the three techniques TDIE, FDTD and TLM has not been made and this work is aimed at filling this gap. It is also hoped that this comparison might help in choosing one method over the other for a given situation.

This paper is organized as follows. In the next three sections, 2,3 and 4, for the sake of completeness, we present a brief description of TDIE, FDTD and TLM methods, respectively. In section 5 the near to far field transformation technique used with FDTD and TLM method is explained. In section 6 numerical results are presented to show the comparison between these three methods. Finally, in section 7, we present the conclusions drawn from this analysis.

2 Formulation of TDIE

Let S denote the surface of an arbitrarily shaped conducting body for which we wish to formulate the time domain scattering problem[5, 12]. An electric field $E^i(r,t)$ defined in the absence of the scatterer, is incident on and induces a surface current $J(r,t)$ on S. The scattered electric field $E^S(r,t)$ computed from the surface current is given by

$$E^S(J) = -\frac{\partial A}{\partial t} - \nabla \Phi, \tag{1}$$

where the magnetic vector potential is defined as

$$A(r,t) = \frac{\mu}{4\pi}\int_S \frac{J(r^{'}, t - R/c)}{R}\mathrm{d}S' \tag{2}$$

and the scalar potential as

$$\Phi(r,t) = \frac{1}{4\pi\varepsilon}\int_S \frac{q_S(r^{'}, t - R/c)}{R}\mathrm{d}S', \tag{3}$$

where $R = |r - r^{'}|$ is the distance between an arbitrarily located observation point r and source point $r^{'}$ on S. In the above expressions, μ and ε are the permeability and permittivity of the surrounding medium, $c = 1/\sqrt{\mu\epsilon}$ is velocity of propagation of the wave in the surrounding medium. The surface charge density q_s is related to the surface divergence of current J through the equation of continuity

$$\nabla_S \square J = -\frac{\partial q_S}{\partial t}. \tag{4}$$

Differentiating Eq. (3) with respect to time and using Eq. (4), we obtain the following expression for the time-derivative of the scalar potential:

$$\Psi(r,t) = \frac{\partial \Phi}{\partial t} = \frac{-1}{4\pi\varepsilon}\int_S \frac{\nabla s \square . J(r^{'}, t - R/c)}{R}\mathrm{d}S'. \tag{5}$$

In Eq. (5) the divergence operator merely differentiates only with respect to the first argument of J and the prime emphasizes that the spatial derivatives are with respect to the primed coordinates. We derive an integro-differential equation for J by enforcing the total tangential electric field to vanish on S, obtaining

$$E^i_{\tan} = \left(\frac{\partial A}{\partial t} + \nabla \Phi\right)_{\tan}, \ r \text{ on } S. \tag{6}$$

The charge density q_s appearing in the scalar potential in Eq. (6) is the time integral of the divergence of the current. To eliminate this integration, we differentiate Eq. (6) with respect to time and use Eq. (5) to obtain

$$\left[\frac{\partial^2 A(r,t)}{\partial t^2} + \nabla \Psi(r,t)\right]_{\tan} = \left[\frac{\partial E^i(r,t)}{\partial t}\right]_{\tan}, \ r \text{ on } S. \tag{7}$$

Eq. (7) with Eq. (2) and Eq. (6) constitutes a time domain electric field integral equation from which the unknown current $J(r,t)$ may be determined. Here we approximate the current on S by

$$J(r,t) = \sum_{k=1}^{N} I_k(t) f_k(r), \tag{8}$$

where I_k is the unknown current coefficient at edge k and N is the number of non-boundary edges. The integrals are then solved by discretizing the body using triangular patches and with the use of Rao-Wilton-Glisson (RWG) basis functions given by

$$f_k(r) = \begin{cases} \frac{l_k}{2A_k^+}\rho_k^+, & \text{for } r \in T_k^+, \\ \frac{l_k}{2A_k^-}\rho_k^-, & \text{for } r \in T_k^-, \\ 0, & \text{otherwise}, \end{cases} \tag{9}$$

where l_k is the length of the edge and $A_k^{\pm}$ is the area of the triangle $T_k^{\pm}$.

Once the current density on the induced scatterer has been obtained, the far scattered field then can be easily computed. The scattered magnetic field at a point r is given by the expression

$$rH^S(r,t_i) = \frac{1}{4\pi c}\sum_{j=-\infty}^{\infty}\sum_{k=1}^{N} I_{k,j},$$

$$\left(\frac{T_j\left(\tau_{k,i+1/2}\right) - T_j\left(\tau_{k,i-1/2}\right)}{c\Delta t}\right)\int_s f_k \times \hat{r}\mathrm{d}S', \tag{10}$$

and with the availability of the far-zone magnetic field, the far-zone electric field can be obtained with

$$E^S(r,t_n) = \eta H^S(r,t_n) \times a_r, \tag{11}$$

where $\eta = \sqrt{\mu/\varepsilon}$ is the wave impedance of the medium surrounding the scatterer.

3 Formulation of FDTD-PML

The FDTD method is a powerful computational tool giving a wide band time-domain data, useful for transient analysis, and can also yield frequency-domain data via Fourier Transforms. The FDTD simulation automatically and self-consistently takes into account the full-wave effects of distributed electromagnetic wave coupling, radiation, ground loops and ground bounce. Given the variety of materials that FDTD can model, very complex and detailed structures may be analyzed with FDTD. The FDTD method uses a system of finite-difference equations for representing the Maxwell's partial differential equations given by

$$\begin{cases} \nabla \times E = -\frac{\partial B}{\partial t} - J_m, \\ \nabla \times H = \frac{\partial D}{\partial t} + J_\varepsilon, \\ \nabla \square D = \rho, \\ \nabla \square B = 0. \end{cases} \tag{12}$$

The finite-difference approximation to any derivative of a function is obtained from the Taylor's series expansion of the function. Normally, the central difference approximation is used because the error for the central difference approximation is of second order. In Yee's method of FDTD calculation, the electric and magnetic field components are interleaved in space and time so as to permit a natural satisfaction of the continuity of the tangential field components at the media interfaces.

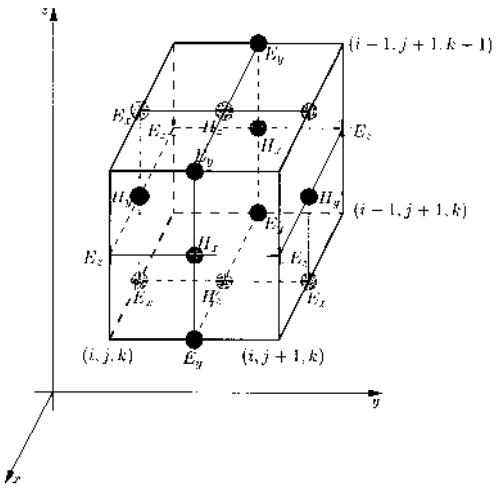

Fig. 1. Interleaving of the electric and magnetic field components at the nodes on a unit cube cell of the space lattice

The Yee's algorithm[14] is implemented by discretizing the object in the Cartesian domain as shown in Fig. 1. The temporal update scheme of one of the components of the electric E and magnetic H fields using Yee's algorithm is given by the following time stepping algorithm:

$$E_x|^n_{i+1/2,j,k} = \left[\frac{1-(\sigma \Delta t/2\varepsilon)}{1+(\sigma \Delta t/2\varepsilon)}\right] E_x|^{n-1}_{i+1/2,j,k} + \left[\frac{\Delta t/\varepsilon}{1+(\sigma \Delta t/2\varepsilon)}\right] \times \left[\frac{H_z|^{n-1/2}_{i+1/2,j+1/2,k} - H_z|^{n-1/2}_{i+1/2,j-1/2,k}}{\Delta y} - \frac{H_y|^{n-1/2}_{i+1/2,j,k+1/2} - H_y|^{n-1/2}_{i+1/2,j,k-1/2}}{\Delta z}\right], \tag{13}$$

$$H_x|^{n+1/2}_{i,j+1/2,k+1/2} = \left[\frac{1-(\sigma^* \Delta t/2\mu)}{1+(\sigma^* \Delta t/2\mu)}\right] H_x|^{n-1/2}_{i,j+1/2,k+1/2} + \left[\frac{\Delta t/\mu}{1+(\sigma^* \Delta t/2\mu)}\right] \times \left[\frac{E_y|^{n}_{i,j+1/2,k+1} - E_y|^{n}_{i,j+1/2,k}}{\Delta z} - \frac{E_z|^{n}_{i,j+1,k+1/2} - E_z|^{n}_{i,j,k+1/2}}{\Delta y}\right], \tag{14}$$

where Δx, Δy and Δz are the spatial steps and Δt is the time step and ε, μ, σ and σ^* are the permittivity, permeability, electrical, and magnetic conductivities, respectively. Expressions for other components of the fields may be written in a similar manner.

The scatterer is irradiated by a plane wave and to implement the plane wave source conditions, the FDTD mesh is divided into a total field region and a scattered field region as shown in the above Fig. 2. The fields in the total field region consist of the sum of the incident plane wave fields and the fields scattered from the

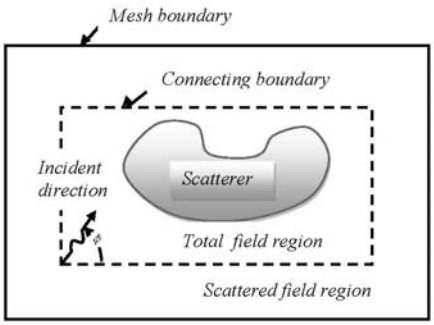

Fig. 2. Separation of mesh into total field and scattered field regions

object under consideration which is completely contained in this region. In the scattered field region, only outward propagating scattered energy is present. The source conditions for the plane wave excitation are enforced on the boundary separating these regions. The procedure consists of adding the known plane wave field contribution to fields passing from the scattered field region to the total field region, and subtracting the plane wave contribution from the fields traveling from the total field region to the scattered field region.

As the Maxwell's equations are hyperbolic in nature, the FDTD is unbounded in one or more of the spatial directions. Thus, to terminate the computational domain, a boundary condition has to be applied. The scattered field FDTD algorithm with PML[2] boundary has been used for computing the electromagnetic interactions presented in this paper. Lastly, we note that for the FDTD case, the time step Δt is chosen using the following criterion, given by

$$c\Delta t = 0.7\left[\frac{1}{\Delta x^2} + \frac{1}{\Delta y^2} + \frac{1}{\Delta z^2}\right]^{-\frac{1}{2}}, \tag{15}$$

where c is the velocity of the electromagnetic wave in free space.

4 Formulation of SCN-TLM

The Transmission-Line Modeling (TLM) method has been successfully applied in the last three decades for the solution of electromagnetic-wave- propagation problems. It is a time domain numerical technique in which both space and time are discretized. The simulation of propagation of electromagnetic waves is done through scattering of impulses in a 3-D meshed network of transmission lines arranged in the form of SCNs[7]. The structure of SCN without stubs is shown in Fig. 3.

The scattering procedure represents the core of the TLM algorithm. The scattering equations relating the voltage pulses on various link lines can be written in a compact form as[13]

$$V^r_{inj} = V_j \pm I_k Z_{inj} - V^i_{ipj} + h_{ij}, \tag{16}$$

$$V^r_{ipj} = V_j \pm I_k Z_{ipj} - V^i_{inj} + h_{ij}, \tag{17}$$

where the upper and lower signs apply, respectively, for indices $(i,j,k)\epsilon\{(x,y,z),(y,z,x),(z,x,y)\}$ and $(i,j,k)\epsilon\{(x,z,y),(y,x,z),(z,y,x)\}$. The factor h_{ij} is given by

$$h_{ij} = \frac{Z_{inj} - Z_{ipj}}{Z_{inj} + Z_{ipj}}\left(V^i_{inj} - V^i_{ipj}\right). \tag{18}$$

The time step of this time stepping algorithm is given by

$$\Delta t = \Delta i\,\sqrt{C_{ij}L_{ij}}, \tag{19}$$

where C_{ij} and L_{ij} are link line distributed capacitance and inductances respectively, Δx, Δy and Δz are node dimensions and $(i,j,k)\epsilon(x,y,z), i \neq j,k$.

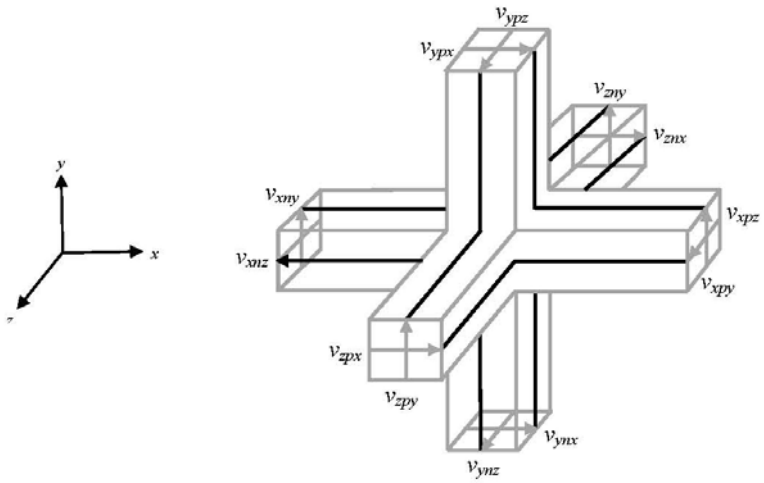

Fig. 3. The Symmetrical Condensed Node (SCN)

The TLM method needs the discretization of the entire simulation space; therefore, directly computing the far scattered field with the method demands prohibitive computational resources. It is necessary therefore to use a near- to far-zone approach combined with an efficient absorbing- boundary condition in order to avoid nonphysical reflections.

As mentioned earlier, the availability of finite computational time and memory resources means that practical implementation of the TLM algorithm requires the use of an artificial truncation of the mesh. But this finite-size mesh stands for an open region, so, if non-physical reflections are to be avoided in the final solution, additional boundary conditions to substitute the eliminated by TLM mesh must be added to the numerical algorithm. The problem of establishing appropriate boundary conditions is a timely one and therefore has been extensively treated in the literature[6, 8]. In the present work, as boundary condition, we used the discrete form of one-way equation combined with a radiation-type condition to reduce mesh size is used. The final expression for the first-order condition used in this paper at the interface, let us say, at $x = 0$ plane is

$$V^{n+1}(0,1,k) = \frac{(d-1)}{3d}\left\{V^{n+1}(1,1,k)+V^{n}(0,1,k) + V^{n}(1,1,k)\right\}. \tag{20}$$

In Eq. (20), $V^n(i,j,k)$ stands for the scattered voltage pulses at spatial point $(i\Delta x, j\Delta y, k\Delta z)$ and time $n\Delta t$, and d is the distance from the nearest point of the scatterer to the boundary point under consideration.

5 Near- to far-field transformation

The FDTD and TLM method needs the discretization of the entire simulation space; therefore, directly computing the far scattered field with the method demands prohibitive computational resources. It is necessary therefore to use a near-to far-zone approach combined with an efficient absorbing-boundary condition in order to avoid non-physical reflections.

When the wave falls over the object,it gets scattered and the far-field data from the FDTD or TLM generated near fields can be obtained by defining a virtual cube surrounding the object with in the mesh. In case of the FDTD method, the cube, on which the electric surface current is calculated, is located at a distance of half the spatial discretization from each of the extremum points of the object along the coordinate axes. The cube for the magnetic surface currents is located at the extremum points of the object. In the case of TLM, the electric and magnetic fields tangential to the cubical surface are calculated at each node lying on this surface. The calculation of electric and magnetic currents is done using

$$J = \hat{n} \times H^s, \tag{21}$$

and

$$M = -\hat{n} \times E^s, \tag{22}$$

respectively. Here, E^s and H^s are the scattered electric and magnetic fields, respectively, and, $\hat{n}$ is the unit outward normal to the virtual surfaces comprising the cube. Then these equivalent currents are integrated with the free space Green's function weighting to obtain far field quantities.

We used a time domain method due Luebbers et al. [10] to implement near to far field transformation. This method involves setting up time dimensioned arrays for the far field vector potentials. Each array element is determined by conducting a recursive sum of contributions from the time domain electric and magnetic current sources just computed via FDTD or TLM on S. These contributions are delayed in time according to the propagation delay between a source element on S and the far field observation point.

6 Numerical results

In this section, we present the numerical results, obtained by irradiating a square plate, a pie plate, a cube and a sphere, all conducting bodies, through TDIE, FDTD and TLM methods. The ideal excitation would be an electromagnetic impulse. However, it is not amenable to numerical solution and hence a smoothed impulse or regularized impulse is being used. An example of a smoothed impulse is Gaussian regularized impulse plane wave, given by

$$E^i(r,t) = a_x 120\pi \frac{4.0}{T\sqrt{\pi}} e^{-\gamma^2}, \tag{23}$$

where

$$\gamma = \frac{4.0}{T}\left[ct - ct_o - r.(-a_z)\right], \tag{24}$$

and E^i is the incident electric field, r is the position vector of the observation point, $T = 4$ lm is the pulse width of the Gaussian impulse, $t_0 = 6$ lm is a time delay that represents the time at which the pulse peaks at the origin, and c is the velocity of propagation of the electromagnetic wave.

As a first example, consider a flat, 2×2 m square plate located in the xy plane and centered about the origin. Eight divisions are made in the x direction and seven in the y direction, resulting in 56 rectangular patches. By joining the diagonals of each rectangle, it results in 112 triangular patches with 153 unknowns. The time step is 0.8434 lm. The storage requirement is 125 KB. As it conforms well to the Cartesian grid, the square plate is the easiest geometry to solve via FDTD. The FDTD-PML space extends to 2.8 m from the origin along x and y directions and $1m$ along the z-direction. It is divided into 56 equal divisions along x and y directions and 20 divisions along the z-direction. The unit cell size is $\Delta x = \Delta y = \Delta z = \Delta l = 5$ cm. For the FDTD solution, it results in 610 766 unknowns and the storage requirement is around 2.2 MB.

The square plate also conforms well to the Cartesian grid and hence it is easy to model the square plate. The TLM space extends to 2.502 m from the origin along x and y directions and 0.834 m along the z-direction. The TLM problem space is divided into 90 equal divisions along x and y directions and 30 divisions along the z-direction. The unit cell size is $\Delta x = \Delta y = \Delta z = \Delta l = 2.78$ cm. For the TLM solution, the time step $\Delta t = \Delta l/2c = 0.0139$ lm. This results in 9 436 036 unknowns and the storage requirement is around 30 MB.

Fig. 4 shows the back-scattered field ($\theta = 0^\circ, \phi = 0^\circ$) and the side-scattered field ($\theta = 90^\circ, \phi = 90^\circ$) for the conducting square plate. We can observe that the solutions from these three methods agree very well.

Next, a pie-shaped plate is considered. This geometry consists of an equilateral triangular plate, 2 m on a side, joined to a semicircular disk with a $2-$ m diameter. The plate lies in the xy plane with the "center" of the disk portion located at the origin. The triangular portion was divided into 36 uniform equilateral patches and the semicircular disk into 20 triangular patches. The discretization resulted in a total of 56 patches with 74 unknowns. The time step is $\Delta t = 0.0777$ lm. And the storage required is 90 KB. For FDTD, the grid is same as that for square plate. Here also the FDTD-PML space extends to 2.8 m from the origin along x and y directions and 1 m along the z-direction. It is divided into 56 equal divisions along x and y directions and 20 divisions along the z-direction. The unit cell size is $\Delta x = \Delta y = \Delta z = \Delta l = 5$ cm. For the FDTD solution, it results in 610 766 unknowns and the storage requirement is around 2.2 MB. For TLM, the grid is same as that

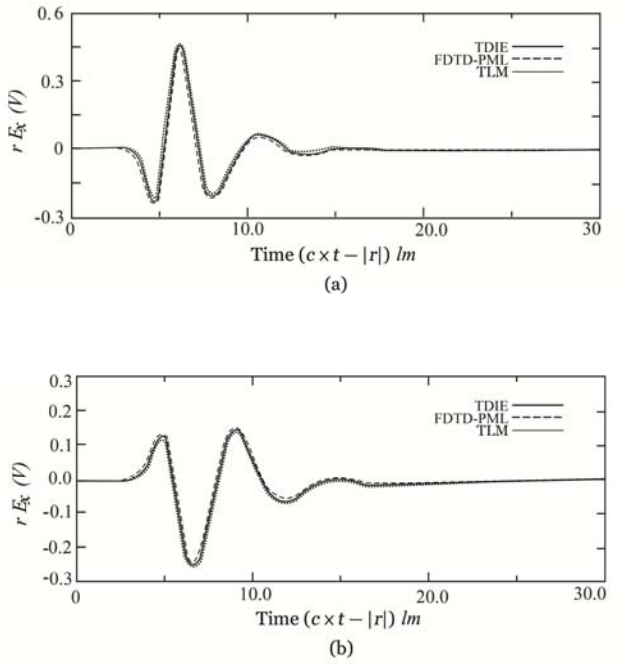

Fig. 4. Far-field response of a conductor square plate of side 2m illuminated by a Gaussian plane wave. (a) Back-scattered field ($\theta = 0^\circ, \phi = 0^\circ$); (b) Side-scattered field ($\theta = 90^\circ, \phi = 90^\circ$)

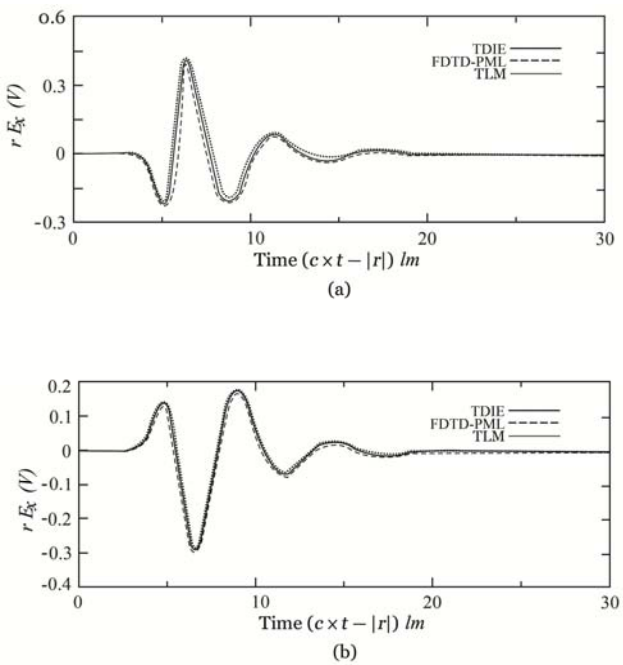

Fig. 5. Far-field response of a conductor pie plate illuminated by a Gaussian plane wave. (a) Back-scattered field ($\theta = 0^\circ, \phi = 0^\circ$); (b) Side-scattered field ($\theta = 90^\circ, \phi = 90^\circ$)

of the square plate i.e. the TLM problem space extends to 2.502 m from the origin along x and y directions and 0.834 m along the z-direction and it is divided into 90 equal divisions along x and y directions and 30 divisions along the z-direction. The unit cell size is $\Delta x = \Delta y = \Delta z = \Delta l = 2.78$ cm. The time step is $\Delta t = \Delta l/2c = 0.0139$ lm. This results in 9 436 036 unknowns and the storage requirement is around 30 MB.

Fig. 5 shows the back-scattered field ($\theta = 0^\circ, \phi = 0^\circ$) and the side-scattered field ($\theta = 90^\circ, \phi = 90^\circ$) for the conducting pie-plate. We can observe that the solutions from these three methods agree very well.

As another example, we considered a conducting cube of side length1.0 m. For the TDIE solution, the surface of the cube is divided into 4, 5, and 5 uniform segments, along the x, y and z directions, respectively. By connecting the diagonals of the resulting patches, a total of 260 triangular patches with 390 unknowns were obtained. Note, that for the TDIE solution, the time-step is $\Delta t = 0.04717$ lm. It required a storage of 640 KB.

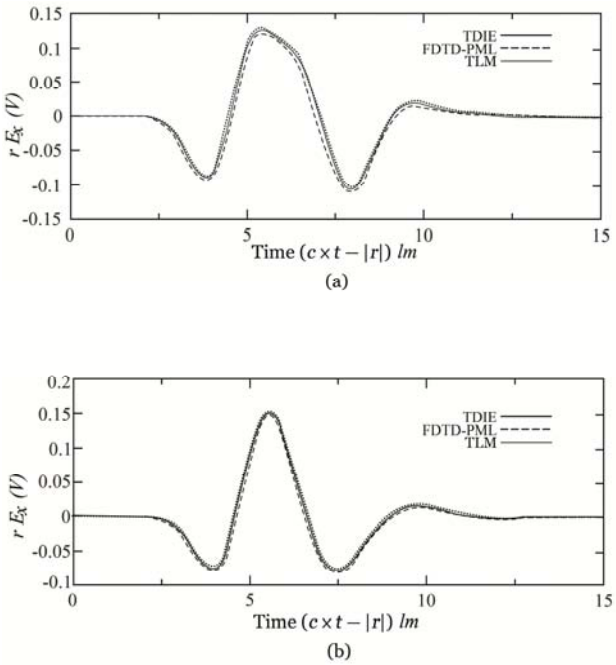

Fig. 6. Far-field response of a conductor cube of side 1.0m illuminated by a Gaussian plane wave. (a) Back-scattered field ($\theta = 0°, \phi = 0°$); (b) Side-scattered field ($\theta = 90°, \phi = 90°$)

The cube is the easiest geometry to solve via the FDTD-PML because it conforms well to the Cartesian grid. The FDTD-PML space extends to 1.9 m from the origin along x, y and z directions and is divided into 38 equal divisions i.e. the unit cell size is $\Delta x = \Delta y = \Delta z = \Delta l = 5$ cm. This results in 534 342 unknowns. The storage requirement is around 2 MB. It is also easy to model the cube via the TLM because it conforms well to the Cartesian grid. The TLM space extends to 1.6667 m from the origin along x, y and z directions and is divided into 60 equal divisions i.e. the unit cell size is $\Delta x = \Delta y = \Delta z = \Delta l = 2.78$ cm. For the TLM solution, the time step is $\Delta t = \Delta l/2c = 0.0139$ lm. This results in 6 609 810 unknowns. As for the computer resources are concerned, the TLM requires nearly 22 MB.

Fig. 6 shows the back-scattered field ($\theta = 0°, \phi = 0°$) and the side-scattered field ($\theta = 90°, \phi = 90°$) for the conducting cube. We can observe that the solutions from these three methods agree very well.

As last example, we considered a conducting sphere with a diameter of 1.0 m. The sphere represents a challenging problem for both the TDIE, FDTD as well as TLM solutions. For all the three solutions we used the stair-stepped approximation of the actual sphere. For TDIE solution, the spherical surface is divided into six divisions along θ direction. Each ring has, starting from the top 13, 27, 29, 29, 27 and 13 patches, respectively. It results in 138 patches total and 207 unknowns. The triangulation is done so that each triangle is closer to equilateral. For the TDIE solution the time step is $\Delta t = 0.0777$ lm. As for the computer resources are concerned, the TDIE requires around 200 KB.

The grid is same as that of the conducting cube. The FDTD-PML space extends to 1.9 m from the origin along x, y and z directions and is divided into 38 equal divisions i.e. the unit cell size is $\Delta x = \Delta y = \Delta z = \Delta l = 5$ cm. This results in 534 342 unknowns. The storage requirement is also same as that of the conducting cube i.e. around 2MB In TLM method, the grid of the cube is used for sphere also. The TLM space extends to $1.6667m$ from the origin along x, y and z directions and is divided into 60 equal divisions i.e. the unit cell size is $\Delta x = \Delta y = \Delta z = \Delta l = 2.78$ cm. For the TLM solution, the time step is $\Delta t = \Delta l/2c = 0.0139$ lm.

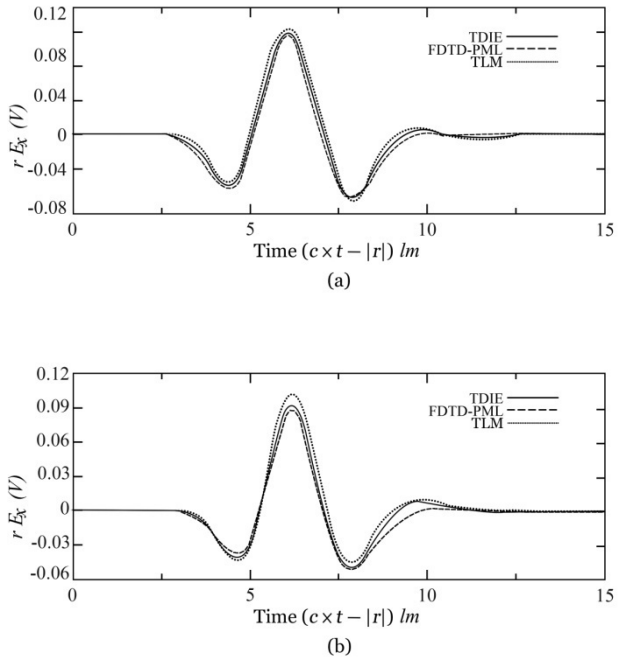

Fig. 7. Far-field response of a conductor sphere of diameter 1.0 m illuminated by a Gaussian plane wave. (a) Back-scattered field ($\theta = 0^\circ, \phi = 0^\circ$); (b) Side-scattered field ($\theta = 90^\circ, \phi = 90^\circ$)

This results in 6 609 810 unknowns. As for the computer resources are concerned, the TLM requires nearly 22 MB.

Fig. 7 shows the back-scattered field ($\theta = 0^\circ, \phi = 0^\circ$) and the side-scattered field ($\theta = 90^\circ, \phi = 90^\circ$) for the conducting sphere. We can observe that the solutions from these three methods agree very well.

Table 1. Comparison of the memory requirements for three methods

Scatterer	TDIE	FDTD	TLM
Square plate	125KB	2.2MB	30 MB
Pie plate	90 KB	2.2 MB	30 MB
Cube	640 KB	2 MB	22 MB
Sphere	200 KB	2 MB	22 MB

The memory requirements of different methods are given in Tab. 1. By observing various graphs presented here, it can be said that despite the vast differences in the modeling philosophies and in the gridding employed by the numerical techniques, all of the techniques provide extremely close solutions.

7 Conclusion

In this paper, we compared TDIE, FDTD and TLM techniques in obtaining the time domain signatures of various conductor bodies with canonical shapes. It can observed that all the three methods generate reasonably accurate solutions for a given discretization scheme. One of the principal advantages of time domain techniques, such as TDIE, FDTD and TLM, is their ability to model the electromagnetic fields in a given geometry over a broad frequency range. One observation we can make is regarding the computer storage requirements: the TLM method demands more when compared to others. The results of this paper can be used to validate or check concurrently one result against the other. Finally, we can also say that the above results are also useful in selecting a particular method that suits to the situation.

References

[1] S. Teflove. The finite difference time domain method. *Computational Electrodynamics, Boston MA, Artech House*, 2000.

[2] J. Berenger. A perfectly matched layer for the absorption of electromagnetic waves. *Journal of Computational Physics*, 1994, **114**: 185–200.

[3] C. Britt. Solution of electromagnetic scattering problems using time domain techniques. *Antennas and Propagation, IEEE Transactions on*, 1989, **37**: 1181–1192.

[4] B. Bennet. Time domain electromagnetics and its applications. **in:** *Proceedings of the IEEE*, 1978, **66**: 299–318.

[5] S. Vechinski. A stable procedure to calculate the transient scattering by conducting surfaces of arbitrary shape. *Antennas and Propagation, IEEE Transactions on*, 1992, **40**: 661–665.

[6] W. Hoffer. The transmission line matrix method-theory and applications. *Microwave Theory and Techniques, IEEE Transactions on*, 1985, (10): 882–893.

[7] P. Johns. A symmetrical condensed node for the TLM method. *Microwave Theory and Techniques, IEEE Transactions on*, 1987, **35**(4): 370–377.

[8] N. Sachdev, S. Rao. Comparison of FDTD-PML with TDIE. *Antennas and Propagation, IEEE Transactions on*, 2002, **50**(11).

[9] R. Johns. Numerical solution of two-dimensional scattering problems using a transmission-line matrix. **in:** *Proceedings of the Institution of Electrical Engineers*, 1971, **118**: 1203–1208.

[10] M. Luebbers, K. Kunz, et al. A finite difference time domain near zone to far zone transformation. *Antennas and Propagation, IEEE Transactions on*, 1991, **39**: 429–433.

[11] S. Rao. *Time domain electromagnetics*. New York: Academic, 1999.

[12] A. Rao, D. Wilton. Electromagnetic scattering by surfaces of arbitrary shape. *Antennas and Propagation, IEEE Transactions on*, 1982, **30**: 409–418.

[13] T. Trenkic, C. Christopoulos. Development of general symmetrical condensed node for the TLM method. *Microwave Theory and Techniques, IEEE Transactions on*, 1996, **44**(12): 2129–2135.

[14] K. Yee. Numerical solution of initial value problems involving Maxwell's equations in isotropic media. *Antennas and Propagation, IEEE Transactions on*, 1966, **AP-14**: 302–307.

[15] W. Chen, M. Ney. Absorbing and connecting boundary conditions for the TLM method. *Microwave Theory and Techniques, IEEE Transactions on*, 1993, **41**: 2016–2024.